

# Lawrence Berkeley National Laboratory

## Recent Work

### Title

EXPERIMENTAL DETERMINATION OF THE KEN PARITY USING A POLARIZED TARGET

### Permalink

<https://escholarship.org/uc/item/9563404z>

### Authors

Dieterle, Byron D.  
Arens, John F.  
Chamberlain, Owen  
et al.

### Publication Date

1967-10-01

*C. Z.*

# University of California

## Ernest O. Lawrence Radiation Laboratory

EXPERIMENTAL DETERMINATION OF THE K $\pi$ N PARITY  
USING A POLARIZED TARGET

Byron D. Dieterle, John F. Arens, Owen Chamberlain,  
Paul D. Grannis, Michel J. Hansroul, Leland E. Holloway,  
Claiborne H. Johnson, Jr., Claude H. Schultz,  
Herbert M. Steiner, Gilbert Shapiro, and David M. Weldon

October 1967

RECEIVED  
LIBRARY AND  
DOCUMENTS SECTION  
OCT 23 1967

**TWO-WEEK LOAN COPY**  
This is a Library Circulating Copy  
which may be borrowed for two weeks.  
For a personal retention copy, call  
Tech. Info. Division, Ext. 5545

UCRL-17230 Rev.

*Cy. Z.*

*E-172*

## **DISCLAIMER**

This document was prepared as an account of work sponsored by the United States Government. While this document is believed to contain correct information, neither the United States Government nor any agency thereof, nor the Regents of the University of California, nor any of their employees, makes any warranty, express or implied, or assumes any legal responsibility for the accuracy, completeness, or usefulness of any information, apparatus, product, or process disclosed, or represents that its use would not infringe privately owned rights. Reference herein to any specific commercial product, process, or service by its trade name, trademark, manufacturer, or otherwise, does not necessarily constitute or imply its endorsement, recommendation, or favoring by the United States Government or any agency thereof, or the Regents of the University of California. The views and opinions of authors expressed herein do not necessarily state or reflect those of the United States Government or any agency thereof or the Regents of the University of California.

Submitted to Physical Review

UCRL-17230 Rev.  
Preprint

UNIVERSITY OF CALIFORNIA  
Lawrence Radiation Laboratory  
Berkeley, California

AEC Contract No. W-7405-eng-48

EXPERIMENTAL DETERMINATION OF THE  $\pi^0$  PARITY  
USING A POLARIZED TARGET

Byron D. Dieterle, John F. Arens, Owen Chamberlain,  
Paul D. Grannis, Michel J. Hansroul, Leland E. Holloway,  
Claiborne H. Johnson, Jr., Claude H. Schultz,  
Herbert M. Steiner, Gilbert Shapiro, and David M. Weldon

October 1967

EXPERIMENTAL DETERMINATION OF THE  $K\Sigma N$  PARITY USING A  
POLARIZED TARGET\*

Byron D. Dieterle,\*\* John F. Arens,\*\*\* Owen Chamberlain, Paul D. Grannis,+  
Michel J. Hansroul,++ Leland E. Holloway,+++ Claiborne H. Johnson, Jr.,  
Claude H. Schultz,† Herbert M. Steiner, Gilbert Shapiro, and David M. Weldon††  
Lawrence Radiation Laboratory, University of California, Berkeley, California

October 1967

ABSTRACT

We have determined the  $K\Sigma N$  parity using the reaction  $\pi^+ p \rightarrow K^+ \Sigma^+$ . A crystal containing polarized protons was used as the target. We have compared the counting rates for events produced from protons polarized parallel and antiparallel to  $\vec{P}_\Sigma$ , where  $\vec{P}_\Sigma$  is the polarization of  $\Sigma$ 's produced from unpolarized protons and has been previously measured. A higher counting rate was obtained for events for which the protons were polarized parallel to  $\vec{P}_\Sigma$ . This means that the  $K\Sigma N$  parity:  $\Pi_{K\Sigma N} = \Pi_{\pi p} = -1$ . This result depends only on the assumptions of spin 1/2 for the sigma and parity conservation in the reaction. The relative probability of odd vs. even  $K\Sigma N$  parity is 21:1. Our result agrees with the usual expectations (as from  $SU_3$ ) and with a previous experimental determination.

---

\* Work done under the auspices of the U. S. Atomic Energy Commission.  
\*\* Present address: SLAC, Stanford University, Stanford, California  
\*\*\* Present address: Goddard Space Flight Center, Greenbelt, Maryland  
+ Present address: State University of New York, Stony Brook, New York  
++ Present address: CEN- SACLAY, Essonne, France  
+++ Present address: University of Illinois, Urbana, Illinois  
† Present address: Columbia University, New York, New York  
†† Present address: Los Alamos Scientific Laboratory, Los Alamos, New Mexico

INTRODUCTION

The method we have used to determine the relative intrinsic parity of the K and  $\Sigma$  particles ( $\Pi_{K\Sigma}$ ) is due to Bilenky,<sup>1</sup> who shows that the differential cross section for production of a  $K\Sigma$  final state by a pion-proton collision is of the form

$$\frac{d\sigma}{d\Omega}(\theta, \phi) = \frac{d\sigma}{d\Omega}(\theta)|_0 (1 + \Pi T P_{\Sigma}(\theta)) \quad (1)$$

$\Pi$  is the product of the initial and final state state intrinsic parities and is equal to  $\Pi_{K\Sigma} \times \Pi_{\pi p}$ . Note that  $\Pi = -\Pi_{K\Sigma N}$ .  $T$  is the component  $(\vec{T} \cdot \hat{n})$  of proton polarization parallel to the normal of the production plane. This normal is taken to be

$$\hat{n} = \frac{\vec{k}_K \times \vec{k}_{\pi}}{|\vec{k}_K \times \vec{k}_{\pi}|}$$

$P_{\Sigma}$  and  $\frac{d\sigma}{d\Omega}|_0$  are the polarization  $(\vec{P}_{\Sigma} \cdot \hat{n})$  and differential cross section for production from an unpolarized proton target. The only assumptions necessary in the derivation of (1) are that parity is conserved and that the  $\Sigma$  has spin 1/2.

At the pion energy and angular region of our experiment and with our definition of  $\hat{n}$ , the average sigma polarization is known to be positive, as determined from experiments with unpolarized targets.<sup>2,3,4</sup>

Complete separation of events produced from polarized protons cannot be made and the final sample of events contains "background" events produced from nucleons bound in complex nuclei in our polarized target. These bound nucleons are not significantly polarized and thus serve only to dilute the effect.

The number of events produced at any angle is the sum of background

events (b) and events from free hydrogen (fh) .

$$\frac{d\sigma}{d\Omega} = \frac{d\sigma}{d\Omega}|_b + \frac{d\sigma}{d\Omega}|_o (1 + I T P_{\Sigma}) .$$

The production cross section for a target whose polarization is in the direction  $\hat{n}$  is

$$\frac{d\sigma}{d\Omega}|_{up} = \frac{d\sigma}{d\Omega}|_b + \frac{d\sigma}{d\Omega}|_o (1 + \Pi |T| P_{\Sigma}) = N_b + N_u$$

For target polarization of the same magnitude, but in the direction  $-\hat{n}$  we have

$$\frac{d\sigma}{d\Omega}|_{down} = \frac{d\sigma}{d\Omega}|_b + \frac{d\sigma}{d\Omega}|_o (1 - \Pi |T| P_{\Sigma}) = N_b + N_d$$

where  $N_b$  is the cross section for  $K^+$  events from non-hydrogen nuclei, and  $N_{u,d}$  is the cross section for  $K^+\Sigma^+$  events from hydrogen.

We now form a quantity  $\epsilon$ , the asymmetry in counting rates for the target polarized parallel and antiparallel to the normal.

$$\begin{aligned} \epsilon &= \frac{\frac{d\sigma}{d\Omega}|_{up} - \frac{d\sigma}{d\Omega}|_{down}}{\frac{d\sigma}{d\Omega}|_{up} + \frac{d\sigma}{d\Omega}|_{down}} = \frac{(N_b + N_u) - (N_b + N_d)}{(N_b + N_u) + (N_b + N_d)} \\ &= \frac{N_u - N_d}{N_u + N_d + 2N_b} = \frac{N_u - N_d}{N_u + N_d} \cdot \frac{N_u + N_d}{N_u + N_d + 2N_b} . \end{aligned}$$

The first term is the asymmetry in counting due to the free hydrogen and the second term is a dilution of the effect due to the presence of background. We can write this as

$$\epsilon = \epsilon' f$$

$$\epsilon' = \frac{N_u - N_d}{N_u + N_d} = \Pi |T| P_{\Sigma}$$

$$f = \frac{N_u + N_d}{N_u + N_d + 2N_b} = \text{fraction of total number of events that come from free hydrogen.}$$

Thus the asymmetry in counting rate  $\epsilon$ , with background included is

$$\epsilon = \Pi |T| P_{\Sigma} f . \quad (2)$$

$|T|$ ,  $P_{\Sigma}$ , and  $f$  are positive so that the sign of  $\epsilon$  determines the  $K\Sigma N$  parity ( $\Pi_{K\Sigma N} = -\Pi$ ). Formula (2) assumes equal magnitudes of polarization for protons polarized in the direction  $\hat{n}$  or  $-\hat{n}$ . The error introduced by using formula (2) is well within the statistical accuracy of this experiment.

## II. EXPERIMENTAL TECHNIQUE

A schematic of the experimental apparatus can be seen in Fig. 1. A beam of 1143 MeV/c  $\pi^+$  was focused on the polarized proton target polarized in a horizontal direction perpendicular to the beam. A  $K^+$  detector placed below the beam line and the polarized target defined a vertical plane of scattering. The detector was sensitive to  $K^+$  of momentum  $370 < P_K < 600$  MeV/c. The detector was designed so that  $K^+$  produced from free hydrogen with c.m. angles  $45^\circ < \theta_{K\pi}^* < 100^\circ$  would stop near the center of the sensitive region of the detector. The sensitive region was a water Cerenkov counter  $C_T$  of inner dimensions 12"x12"x14" which counted the fast decay products of the  $K^+$ .

$$K^+ \rightarrow \mu^+ \nu \quad \text{BR (Branching Ratio)} \sim 63\%$$

$$K^+ \rightarrow \pi^+ \pi^0 \quad \text{BR} \sim 21\%$$

Upon electronic detection of a stopping  $K^+$ , spark chambers were fired and photographed to record the trajectories of the  $K^+$  and its decay products as well as the incident  $\pi^+$  trajectory.

The asymmetry of counting rates for  $K^+ \Sigma^+$  produced from free hydrogen polarized parallel or antiparallel to  $\hat{n}$  gives the  $K\Sigma$  parity when Eq. 2 is used.



A. Beam

Figure 2 shows a diagram of the beam which was produced from an aluminum internal target placed in the north tangent tank straight section of the Bevatron. A bending magnet M1 induced momentum dispersion at focus 1 where a copper slit served to select a momentum band. At focus 2 the momentum dispersion was partially cancelled. A 20 ft. long velocity spectrometer with crossed DC electric and magnetic fields caused the  $\pi^+$  and protons to be separated by about .6" at focus 2. A 4" copper bar at  $f_2$  intercepted the protons but not the pions. The pions were refocused downstream onto the polarized target at focus 3. Momentum dispersion was removed at  $f_3$  by bending magnet M4. Accurate wire orbits were made between  $f_1$  and  $f_2$  and the remaining magnets were tuned empirically to maximize coincidences of 1/4" square counters temporarily placed at  $f_1$ ,  $f_2$ , and  $f_3$ . The  $\pi^+$  beam momentum was obtained by correcting the wire orbit momentum by the amount of energy lost by a  $\pi^+$  traversing material in the beam. The resulting beam momentum at the center of the target was 1143 MeV/c and had a spread of  $\pm 14$  MeV/c as determined by measurement of  $\pi^+$  tracks in the beam spark chambers. The beam spot at  $f_3$  was about 1.3" in diameter. Angular divergence in the vertical and horizontal planes was  $\pm .6^\circ$  and  $\pm 1.2^\circ$  respectively.

The maximum beam achieved was 400,000  $\pi^+$  per pulse with  $2 \times 10^{12}$  protons on the production target. Typical beam intensity during the experiment was 250,000  $\pi^+$  per pulse with a beam spill of 600 ms duration.

### B. Polarized Target

The target consisted of four crystals of  $\text{La}_2\text{Mg}_3(\text{NO}_3)_{12} \cdot 24 \text{H}_2\text{O}$  with nominally 1% of the La replaced by Neodymium<sup>142</sup>. The free hydrogen in the water of hydration was 3.2 percent by weight of the target which overall had a density of 2 and weighed 19.2 grams. The free hydrogen was polarized by the process of dynamic nuclear orientation which has been described in detail by other authors.<sup>5</sup>

Our target was operated in a field of 18.4 Kg at a temperature of 1.2°K, and irradiated with about one watt of 70 GHz microwaves. The polarization averaged 47% during the experiment. Polarization was reversed by changing the microwave frequency by 0.2%. Because the magnetic field was not changed, the geometry of the experiment was the same for both polarizations. Proton polarization was reversed every 2 hours following He<sup>4</sup> refills of the cryostat.

### C. Detection

An event of interest consisted of a single  $\pi^+$  incident on the polarized target coincident in time with a  $K^+$  emerging from the target and stopping in the  $K^+$  telescope.  $\pi^+$  were identified electronically with scintillation counters in the beam. For the beam, the coincidence logic was

$$\pi^+ = B_1 B_2 \bar{A}_{\text{hole}}$$

with  $B_1$  a scintillation counter at focus 2 ( $f_2$ ), similarly  $B_2$  at  $f_3$ , forming a time-of-flight coincidence which eliminated protons remaining after the separator.  $A_{\text{hole}}$  was a scintillation counter having a 1.5"-diameter hole and placed in front of the target to veto  $\pi^+$  not incident on the region of the target.

$K^+$ 's were identified by a  $K^+$  telescope consisting of copper degrader, Cerenkov counters, scintillators and spark chambers arranged as in Figs. 1 and 3. The copper degrader was a different thickness for each of the three adjacent  $S_2$  counters. These thicknesses were chosen to stop the  $K^+$  originating from free hydrogen near the center of the 12" x 12" x 14" Cerenkov counter  $C_T$ . The  $K^+$  telescope was sensitive to elastic  $K^+\Sigma^+$  events with center-of-mass angles (c.m.)  $45^\circ < \theta_{K\pi}^* < 100^\circ$ .  $K^+$  outside the interval  $370 \text{ MeV}/c < p_K < 610 \text{ MeV}/c$  did not stop in  $C_T$ .

For the purpose of spark chamber triggers a  $K^+$  was defined to be a slow ( $\beta < .75$ ) particle incident on  $C_T$  at time zero followed by a fast particle ( $\beta > .75$ ) emerging from  $C_T$  in the time interval 6-50 ns. This signified the decay of a stopped  $K^+$ . Thus the logic used to signal electronically a possible stopped  $K^+$  was the following:

$$K^+_{\text{stop}} = (S_1 S_2 S_3 \bar{C}_1 \bar{C}_2) \cdot (C_T \text{ MU})_{\text{delayed 6-50 ns}}$$

where  $S_2$  denotes any of the three  $S_2$  counters and MU denotes any of the four  $\mu$  counters. Spark chambers were fired by the logic pulse

$$\text{Trigger} = \pi^+ K^+_{\text{stop}} \overline{\text{DIPR}} \overline{\text{PILEUP}}$$

DIPR (double incident particle rejector) vetoed if two beam particles came within 450 ns and helped protect the  $K^+$  telescope from accidental coincidences. PILEUP integrated the beam and vetoed if the beam spark chambers had  $\geq 4$  tracks within their sensitive time of about 1  $\mu$ s.

Final identification of  $K^+$  events was made by measurements of the spark-chamber tracks which were recorded on film. The intersection of the decay track of the mu spark chamber and the incident particle track in  $K^+$  determined the range of the stopping particle. The momentum was obtained

by tracing orbits through the magnetic field surrounding the target and fitting these orbits to the tracks in K1, K2, and K3. If the momentum was within 100 MeV/c of the momentum obtained from  $K^+$  range tables, the particle in the telescope was accepted as a  $K^+$ . The  $\pi$ , K and proton curves of momentum vs. range differ by more than 100 MeV/c for the band of ranges accepted by our detector. Because of the momentum resolution ( $\sim 15\%$ ), a more stringent cutoff could have removed valid events. This criterion was sufficient to give a very pure sample of K mesons.

The electronic requirements for a trigger were sufficiently lax so that only  $\sim 10$  percent of the pictures had a genuine  $K^+$  in the  $K^+$  telescope. This 10 percent had a time distribution of decay products in agreement with the 12 ns  $K^+$  lifetime. The time distribution in Fig. 4 shows no excess events at early time ("prompts"). The lack of "prompts" confirms that we have a clean  $K^+$  sample.

A complete investigation into the causes of the electronic triggers which did not involve an identifiable  $K^+$  was not undertaken. However, the same  $K^+$  detector was used in a subsequent experiment of a similar nature<sup>6</sup> in which the detector was more closely studied. Both this experiment and the later experiment agreed on the basic characteristics of the  $K^+$  detector. Two separate classes of event triggers existed and these comprised the bulk of the events in which a  $K^+$  could not be identified. Fifty percent of the pictures had no track in the mu chamber. These events could be explained as due to particles which hit a mu counter but missed the spark chamber. Many of these events had a small pulse in the mu counter which could have been due to Cerenkov radiation from a particle

passing through its light pipe. In addition, the requirement that 3 gaps of a mu chamber fire meant roughly one of four particles hitting the scintillator portion of a mu counter missed the spark chamber. A rough calculation of the solid angles involved is in agreement with this interpretation for events having no track in the mu chambers. The remainder of the false triggers were mainly prompt events. Most of these triggers were found to be due to protons. These triggers are thought to be caused by protons of  $\beta \sim .8$  which did not fire Cerenkov veto-counters  $C_1$  and  $C_2$  ( $\beta_{\text{thres}} = 0.75$ ) then fired Cerenkov counter  $C_T$  and a mu counter. Although the ( $\mu - C_T$ ) coincidence for these events must be delayed 6 ns from true prompts to result in a trigger, time jitter due to the physical size of the mu counter (5 ns) and electronic effects such as discriminator time slewing would allow some coincidences. A redesign of the  $K^+$  detector could eliminate most of the above false triggers, but would involve protecting the mu counter light pipes. Accidental triggers are negligible for our experiment.

The time distribution was obtained by measuring the time separation of the S3 and  $\mu$  scintillator pulses. All important counter pulses were displayed on a 4-beam oscilloscope and photographed each time the spark chambers fired. Periodic scans of this film were made during the run to check the electronics.

The  $\pi^+$  trajectory was determined by four spark chambers in the beam. Two were upstream of bending magnet M4 and two were downstream. About 65 percent of the events involving  $K^+$  had tracks in  $B_1 B_2 B_3 B_4$  of sufficient quality to reconstruct the  $\pi^+$  momentum.

Tables I and II give a list of the counters and spark chambers used in the experiment.

#### IV. DATA ANALYSIS

Film accumulated during the experiment contained alternate blocks of data that were taken with positive target enhancement and negative enhancement. Here positive enhancement means that polarization was in the direction of the magnetic field which, for our geometry, was in the direction opposite to the normal of the scattering plane  $\hat{n}$ . Data taken with positive enhancement will often be called + data in the following text.

The data was scanned in a manner designed to equalize efficiency for the + and - data. Events selected for measurement were then measured on the SCAMP measuring-projector system at Berkeley. These events were analyzed on a 7094 computer with a program, SHERLOCK, that identified events having a genuine  $K^+$  in the detector. Further analysis and cutoffs to remove  $K^+$  events of low quality were done with program SUMX.

##### A. Scanning and Measuring

Blocks of + and - data taken near to each other in time during the experiment were scanned together on a dual projector machine. Twenty frames of + data were alternated with twenty frames of - data and the roll and frame numbers of events to be measured were recorded as encountered. Thus, each scanner selected events from equal amounts of + and - data. The alternation between the + and - data was to eliminate

Table I. Details of counters. Counters labeled C are water filled Cerenkov counters and the rest are scintillation counters.

Counter	Dimensions	Photomultipliers	Remarks
S <sub>1</sub>	10" × 10" × $\frac{1}{2}$ "	C70101	
S <sub>2A</sub>	10" × 2" × $\frac{1}{2}$ "	7264	
S <sub>2B</sub>	10" × 2 $\frac{1}{2}$ " × $\frac{1}{2}$ "	7264	
S <sub>2C</sub>	10" × 3 $\frac{1}{2}$ " × $\frac{1}{2}$ "	7264	
S <sub>3</sub>	11" × 11" × $\frac{1}{2}$ "	Two 7850's	
A <sub>hole</sub>	16" × 3 $\frac{1}{2}$ " × $\frac{3}{4}$ " with 1 $\frac{1}{2}$ " diam hole	6810A	
DIPR	5" diam $\frac{1}{4}$ " thick	6810A	
C <sub>1</sub>	12 $\frac{1}{8}$ " × 12 $\frac{1}{8}$ " × 2 $\frac{3}{8}$ "	Six 6655A's	Wavelength shifter added
C <sub>2</sub>	12 $\frac{1}{8}$ " × 12 $\frac{1}{8}$ " × 2 $\frac{3}{8}$ "	Six 6655A's	Wavelength shifter added
C <sub>T</sub>	14 $\frac{1}{2}$ " × 12 $\frac{1}{2}$ " × 14 $\frac{1}{2}$ "	Four 58AVP's	Lined with M <sub>g</sub> O
μ <sub>2</sub> , μ <sub>4</sub>	16 $\frac{3}{8}$ " × 16 $\frac{3}{8}$ " × $\frac{3}{8}$ "	7850	
μ <sub>1</sub> , μ <sub>3</sub>	18 $\frac{3}{4}$ " × 16 $\frac{3}{8}$ " × $\frac{3}{8}$ "	7850	
B <sub>1</sub>	2 $\frac{1}{2}$ " × 1 $\frac{1}{4}$ " × $\frac{1}{4}$ "	7746	
B <sub>2</sub>	3 $\frac{1}{2}$ " diam × $\frac{1}{4}$ " thick	7746	

Table II. Details of spark chamber construction.

Chamber	Dimensions	Gaps	Plate thickness	Remarks
B <sub>1</sub> , B <sub>2</sub> , B <sub>3</sub> , B <sub>4</sub>	8" x 8" x 2"	Eight $\frac{1}{4}$ "	2 mil Al.	Two dummy gaps
B <sub>5</sub>	2" x 1 $\frac{1}{2}$ " x $\frac{1}{2}$ "	Two $\frac{1}{4}$ "	1 mil Al.	
K <sub>1</sub>	Front face 9" x 3"	Twelve $\frac{1}{4}$ "	1 mil Al.	
	Back face 9" x 1 $\frac{1}{2}$ "			
	Thickness 3"			
K <sub>2</sub>	7" x 7" x 1 $\frac{1}{2}$ "	Six $\frac{1}{4}$ "	2 mil Al.	Two dummy gaps
K <sub>3</sub>	10" x 10" x $\frac{1}{2}$ "	Six $\frac{1}{4}$ "	2 mil Al.	
K <sub>4</sub>	14" x 12" x 3"	Eight $\frac{3}{8}$ "	2 mil Al.	
MU <sub>2</sub> , MU <sub>4</sub>	14 $\frac{1}{4}$ " x 14" x 13"	Eight $\frac{3}{8}$ "	2 mil Al.	
MU <sub>1</sub> , MU <sub>3</sub>	16 $\frac{1}{4}$ " x 14" x 3"	Eight $\frac{3}{8}$ "	2 mil Al.	

All chambers filled with 90% Ne, 10% He



biases due to scanner fatigue. Projector 1 and 2 of the dual beam projector were randomized between + and - data without the knowledge of the scanner. Because 95% of the  $K^+$ 's are produced from non-hydrogen nuclei, the number of events selected from the + data and - data should be nearly equal. This was found to be the case and serves as a check on the relative efficiency for identifying events in the + and - data.

Events were selected for measurement by the following criteria:

1.  $K_2$ ,  $K_3$  and  $K_4$  had one and only one track in them;
2.  $K_1$  chamber had one and only one "down" track, meaning a particle that was inclined downward to the horizontal plane;
3. At least one of the four mu chambers had a track; and
4. One and only one  $S_2$  counter fired.

A track was defined to be  $\geq 2$  sparks in the chamber with the exception that  $\geq 3$  sparks were required for  $K_4$  and the mu chambers. The  $K_1$  chamber had alternate gaps displayed in separate views. For this chamber each split view was treated as a separate chamber and criteria (1) through (4) applied. An event was accepted if one or both split K chamber views showed the "down" track.

Measurement of the events selected by scanning was done on the SCAMP machines at Berkeley without attempting to equalize the amounts of + and - data each scanner handled. On these machines the cross hair was adjusted manually to give the best visual fit to sparks in the chamber gaps and the  $\theta$ , X, and Y film coordinates were recorded on magnetic tape.

Computer analysis with SHERLOCK reconstructed the event in three

dimensions from the SCAMP film coordinates and identified events involving a  $K^+$ .

Because good kinematic resolution was important, more stringent cutoffs were later made. The final  $K^+$  sample satisfied the following requirements:

1. The  $K^+$  trajectory intersected the target crystal;
2. Range-momentum and the curvature momentum agreed within 100 MeV/c;
3. The  $K^+$  track in  $K^4$  intersected the decay track of the mu chamber within 1.25", and this intersection was inside  $C_m$ ; and
4.  $K^+$  tracks in chambers  $K1$  through  $K4$  fitted a continuous trajectory.

The total kinematic information obtained from the spark chambers and electronics was the following:

1. Identification of  $\pi^+$  by time of flight,
2. Momentum  $\vec{p}_\pi$  of the  $\pi^+$ ,
3. Identification of  $K^+$ , and
4. Momentum  $\vec{p}_K$  of  $K^+$  (best determined from observed range and checked with curvature in the magnetic field).

Information could not be obtained directly from Sigmas which decayed before reaching the  $K1$  spark chamber. However both the events of interest and the background events can result in an additional particle being present in spark chamber  $K1$  via the decays:

$\Lambda \rightarrow p\pi^-$	BR = 67%
$\Sigma^0 \rightarrow \Lambda\gamma$	BR = 100%
$\quad \quad \quad \downarrow$ $\quad \quad \quad \rightarrow p\pi^-$	BR = 67%
$\Sigma^+ \rightarrow p\pi^0$	BR = 50%
$\Sigma^+ \rightarrow n\pi^+$	BR = 50%.

The last mode has a small solid angle for detection in K1. In the other decays the protons are kinematically constrained to be within about  $20^\circ$  of the hyperon direction. If the assumption is made that the  $K^+$  was produced from a free proton, the  $\Sigma^+$  direction can be predicted and compared to the observed proton direction. We call the angle between the  $\Sigma$  and proton directions  $\theta_{\Sigma p}$  and define  $\theta_{\max}$  as the maximum value one can have for  $\theta_{\Sigma p}$  assuming the event occurred on free hydrogen.

The answers to the two questions

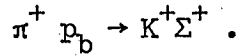
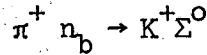
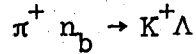
1. Is there an additional track in K1?
2. If so is  $\theta_{\Sigma p} < \theta_{\max}$  ?

were used to label events. All subsamples of events selected in this manner either gave no improvement in the data or contained too few events to be statistically significant. The final result did not use this selection.

For a given incident pion momentum  $K^+\Sigma^+$  events produced from free hydrogen will have a definite relation between  $|\vec{p}_K|$  and  $\theta_K$  given by the two-body kinematics. This relation can be used to eliminate a large fraction of the background events involving  $K^+$  produced by other reactions. In the next section we describe the sources of background events and the means for reducing background.

### B. Background

Because the target was composed of only 3.2 percent hydrogen by weight a large number of  $K^+$  arose from  $\pi^+$  interactions in the heavier nuclei. The main background reactions were from bound neutrons ( $n_b$ ) and bound protons ( $p_b$ ) :



In general bound nucleons have Fermi momenta  $|\vec{p}_F| \sim 200 \text{ MeV}/c$ . Hence the  $K^+$  produced from these nucleons will not usually have  $p_K$  and  $\theta_K$  that agree with the two-body kinematics as calculated for free protons. We wish to select those events that are consistent with the kinematics of the desired reaction,  $\pi^+ p \rightarrow K^+ \Sigma^+$ . In order to make the selection it is necessary to calculate for each interesting event a parameter that tells how far the particular event deviates from the kinematic momentum-angle relation. There are many satisfactory ways of doing this. We have chosen a particular method, as follows. In effect we pretend that each event occurs on a free target proton and calculate the "missing mass" of a presumed unobserved hyperon. Where the observed  $K^+$  does not fit the kinematics of the desired reaction, the so-called missing mass, called  $m$  in our formalism, deviates from the sigma mass  $m_\Sigma$ . For the desired events the values of  $m$  cluster around the value  $m_\Sigma$ .  $m$  is calculated from the relation:

$$m^2 = (E_\pi + m_p - E_K)^2 - (\vec{p}_\pi - \vec{p}_K)^2 .$$

For each event the quantity  $m$  was calculated and entered in a histogram so the distribution of  $m$  values could be displayed. This "mass" distribution should show a peak centered at  $m = m_\Sigma$  corresponding to events produced from free hydrogen in the crystal. Figure 5 shows the mass distribution of events produced from the polarized proton target. No peak due to hydrogen events is observed at the mass  $m_\Sigma$ .

because the peak is obscured by a large background.

To aid the separation of background, data were taken with  $\text{CH}_2$  in place of the crystal. In the data taken with  $\text{CH}_2$ , which effectively has four times more hydrogen per unit mass, the hydrogen peak stood sufficiently above background events to allow an estimate of its position and width. In addition the ratio of peak to background events in  $\text{CH}_2$  allowed us to an estimate of this ratio for the crystal.

In principle, one might expect some background from 3-body final states such as  $\text{K}^+\Lambda\pi$  and  $\text{K}^+\Sigma\pi$ . However the contribution of these events is negligible. The experiment was operated at an energy lower than the threshold for producing these events in free hydrogen. While 3-body states might still be produced in collisions on bound nucleons, the cross section for this process is known to be small ( $\lesssim 10 \mu\text{b}$  as compared to  $200 \mu\text{b}$  for the desired reaction), and what few events there are must be spread thinly over a large range of the parameter  $m$ . The mass distribution for  $\text{CH}_2$  data is shown in Fig. 6. Table III gives summaries of the data taken with  $\text{CH}_2$  and crystal targets. Some data was taken with a target material chosen to approximate the crystal target composition without hydrogen. The distribution of these events vs.  $m$  has a shape outside the peak consistent with the shape of the data taken with the Xtal target and  $\text{CH}_2$  target. The number of events obtained from this "dummy" target is too small to make a direct determination of background in the peak region of the crystal data.

#### $\text{CH}_2$ Data

The events observed with the  $\text{CH}_2$  target in place were treated in

Table III. Summary of data.

Target	Target Wt	Target polarization	No. of $\pi^+$	No. of $K^+$ events	Events in peak region (1190 $\pm$ 6 MeV)	Events in peak produced from protons
CH <sub>2</sub>	~ 13 g	0	$1.4 \times 10^9$	246	88	~ .54
XTAL	19.2	+	$1.0 \times 10^{10}$	1165	237	
		-	$0.96 \times 10^{10}$	1090	261	
		sum of + and -	$1.96 \times 10^{10}$	2255	498	~ .22*

\* Based on CH<sub>2</sub> data

a fashion similar to events with the polarized target and a histogram of the values of  $m$  was formed, as shown in Fig. 6. The peak due to free hydrogen events stands out clearly. The background does not center at the sigma mass for several reasons.  $K^+\Lambda$  events preferentially populate the lower mass region because  $m_\Lambda < m_\Sigma$ .  $K^+\Sigma$  events are shifted to low missing mass by the kinematics of collisions with nucleons bound in the potential well of a nucleus. The resolution of the  $K^+$  detector also favors low mass values to some extent.

On the basis of this histogram we chose the range

$$1184 \text{ MeV} < m < 1196 \text{ MeV}$$

as the band of  $m$  values to be used for the calculation of results (for the polarized-target data).

In the region of 1190 MeV the  $\text{CH}_2$  data of Fig. 6 shows a peak with approximately equal amounts of background and free hydrogen events. To confirm our interpretation of the histogram we have performed a Monte Carlo calculation of the distribution to be expected from collisions on bound nucleons in carbon. A Fermi model of the nucleus was used to estimate the  $K^+$  production angular distribution, and the detection efficiency of our apparatus was folded in. The dashed line on Fig. 6 shows the result of the calculation, normalized to the experimental data. The shape fits the data fairly well and confirms our observation of roughly equal amounts of peak and background events in the chosen band. From the Monte Carlo calculation we estimate the background to be  $40 \pm 7$  events out of the total of  $88 \pm 10$  events in the peak. This gives a ratio of hydrogen events to background events

$$r_{\text{CH}_2} = \frac{\text{No. free}}{\text{No. bkgd}} = \frac{88 \pm 10}{40 \pm 7} - 1 = 1.20 \pm .46$$

If we assume that heavy nuclei have reaction cross sections proportional to  $A^{2/3}$  we can scale the quantity  $r_{\text{CH}_2}$  to the polarized crystal which has an average  $A_{\text{XTAL}} = 19$

$$\begin{aligned} r_{\text{XTAL}} &= r_{\text{CH}_2} \left( \frac{\% \text{ hydrogen}}{\% \text{ heavy elements}} \right)_{\text{XTAL}} \left( \frac{\% \text{ carbon}}{\% \text{ hydrogen}} \right)_{\text{CH}_2} \left( \frac{A_{\text{XTAL}}}{A_{\text{CARBON}}} \right)^{1/3} \\ &= (1.20 \pm 0.46) \left( \frac{.032}{.968} \right) \left( \frac{12}{2} \right) \left( \frac{19}{12} \right)^{1/3} \end{aligned}$$

$$r_{\text{XTAL}} = 0.28 \pm .11$$

which yields

$$f = \frac{r_{\text{XTAL}}}{1+r_{\text{XTAL}}} = 0.215 \pm .065$$

This estimate depends only weakly on our use of the  $A^{2/3}$  screening law. Using this value of  $f$ , the average target polarization

$$|T|_{\text{ave}} = 0.47 \pm 0.10$$

and the average sigma polarization taken from bubble chamber experiments, we can now calculate the expected value of the raw asymmetry,  $\epsilon_{\text{pred}}$ , to be observed in this experiment.

$\langle P_{\Sigma} \rangle$  was obtained, using the angular distribution coefficients of Doyle, Crawford, and Anderson<sup>2</sup> at 1170 MeV/c, and averaging over the angular interval ( $45^\circ < \theta_K^* < 100^\circ$ ) of this experiment. Although these data refer to slightly different energies,  $P_{\Sigma}$  varies slowly in this energy region, and is always positive. One finds  $\langle P_{\Sigma} \rangle = -0.435 \pm 0.13$ .



Thus the expected raw asymmetry

$$\epsilon_{\text{pred}} = \langle P_{\Sigma} \rangle \cdot |T| \cdot f = - .044 \pm .021$$

if  $K\Sigma N$  parity is odd, and with the opposite sign if even.

The  $\text{CH}_2$  data of Fig. 6 show most of the events produced from free hydrogen to be contained in the band of  $m$  values 12 MeV wide. This indicates our resolution in  $m$  for the  $\text{CH}_2$  data of the order of 6 MeV or less. Calculation shows that the resolution for the polarized target data is of the same order of magnitude.

For each event the quantities  $\pi = |\vec{p}_{\pi}|$ ,  $k = |\vec{p}_k|$ ,  $\theta = \cos^{-1} \frac{\vec{p}_{\pi} \cdot \vec{p}_k}{\pi k}$  have errors which contribute to the resolution width. A calculation of the resolution for a typical event gives the rms error in the parameter  $m$

$$\overline{\delta m^2} = \overline{\Delta_{\theta}^2} + \overline{\Delta_{\pi}^2} + \overline{\Delta_K^2} - 2\overline{\Delta_K \Delta_{\pi}} + \text{very small cross terms where } \Delta \text{ denotes the contribution of a particular measurement error.}$$

$$\overline{\delta m^2} = 14.1 + 16.4 + 5.2 - 4.3$$

$$\delta m_{\text{rms}} = \pm 5.7 \text{ MeV}$$

This can vary by about  $\pm 10\%$  for other events contained in our sample.

The largest contribution to the resolution width comes from the uncertainty in the momentum measurement of the incoming pion. Since our estimates rest on somewhat arbitrary assumptions in any case we have chosen 6 MeV as our resolution for  $m$ . Any error in this width does not affect our conclusions but may change the confidence level somewhat.

## V. RESULTS

Figure 5 shows the missing mass distribution for data taken with the target protons polarized positive and negative. Data taken with negative

target polarization were multiplied by 1.12 before plotting, to give equal areas outside the region  $1190 \pm 6$  MeV. The error in this factor due to statistics alone is about 5%. If we had used beam monitors to normalize, this factor would have been 1.04. In the bin corresponding to missing mass =  $m_{\Sigma}$  there is an excess of events for the data taken with negative target polarization. Figure 7 shows a plot of the asymmetry  $\epsilon = \frac{(N^+ - N^-)}{(N^+ + N^-)}$  for each 12-MeV bin. The asymmetry in the bin centered at 1190 MeV corresponds to greater counting rate for  $K^+\Sigma^+$  production from protons polarized parallel to the sigma polarization direction  $\vec{P}_{\Sigma}$  (as found in references 2 and 4). This is in agreement with odd  $K\Sigma N$  relative parity. Figure 8 is a similar plot with 4-MeV-wide bins using the same data.

The asymmetry we measure is an average over the production angles  $45^\circ < \theta_K^* < 100^\circ$ . Its value is calculated from the data of Table III.

$$\begin{aligned} \epsilon_{\text{exp}} &= \frac{237 - 1.12 (261)}{237 + 1.12 (261)} \\ &= -0.104 \pm .050 . \end{aligned}$$

The error shown is statistical, including the 5% uncertainty in the normalization factor.

Figure 9 shows the comparison of  $\epsilon_{\text{exp}}$ , and the  $\epsilon_{\text{pred}}$  calculated above, with the theoretical possibilities allowed for the cases  $\Pi_{K\Sigma N} = \pm 1$ . The experimental point lies 1.1 standard deviations from the nearest point on the line corresponding to odd  $K\Sigma N$  parity, and 2.7 standard deviations from the nearest point on the line corresponding to even  $K\Sigma N$  parity. The ratio of probabilities for these two cases is 21:1.

This result agrees with the prediction of Unitary Symmetry which places the K meson in a pseudoscalar octet and the  $\Sigma$  hyperon in the octet

of  $J^{\text{Parity}} = 1/2^+$ . Previous experiments to determine the  $\Sigma\Lambda$  and  $K\Lambda$  parity<sup>7,8</sup> have been performed with the result that  $\Pi_{\Sigma\Lambda} = +1$  and  $\Pi_{K\Lambda} = -1$ , which indirectly agrees with our result  $\Pi_{K\Sigma} = \Pi_{K\Lambda} \Pi_{\Sigma\Lambda} = -1$ . An earlier experimental determination of  $K\Sigma$  parity was made by Tripp et al.<sup>9</sup> using an energy dependent phase shift analysis to analyze the reaction  $K^- p \rightarrow Y_0^*(1520) \rightarrow \text{all channels}$ . Their result, which is less free of assumptions, was also in agreement with negative  $K\Sigma$  parity.

ACKNOWLEDGMENTS

The authors would like to thank the accelerator technicians for building the counters and spark chambers, and the Bevatron crew and electronic technicians for their help during the data taking. Other support groups, scanners, and summer students assisted in the various phases of the experiment and we thank them as well.

Dr. Mafuzel Huq participated during part of the run and when the experiment was in the early planning stage, Dr. Ludwig Van Rossum contributed some interesting ideas.

REFERENCES

1. S. M. Bilenky, Nuovo Cimento 10, 1049 (1958).
2. Joseph C. Doyle, Frank S. Crawford, Jared Anderson, UCRL-17703, submitted to Phys. Rev.; Frank S. Crawford, Fernand Grand, Gerald A. Smith, Phys. Rev. 128, 368 (1962).
3. Roger O. Bangerter, Angela Barbaro-Galtieri, J. Peter Berge, Joseph J. Murray, Frank T. Solmitz, M. Lynn Stevenson, and Robert D. Tripp, Phys. Rev. Letters 17, 495 (1966).
4. Bruce Cork, Leroy Kerth, W. A. Wenzel, James W. Cronin, R. L. Cool, Phys. Rev. 120, 1000 (1960).
5. C. D. Jeffries, Dynamic Nuclear Orientation (Interscience Publishers, New York, 1963); G. Shapiro, Prog. Nucl. Tech. Instr. (North-Holland) 1, 173 (1964); Claude H. Schultz (Ph. D. thesis), UCRL-11149 Jan. 1964.
6. David M. Weldon, Measurement of the Polarization of the  $\Sigma^-$  in the Process  $\pi^- p \rightarrow \Sigma^- K^+$ , (Ph. D. thesis) UCRL-17152, Dec. 1966 (to be published).
7. H. Courant, H. Filthuth, P. Franzini, R. Glasser, A. Minguzzi-Ranzi, A. Segar, W. Willis, R. Bernstein, T. Day, B. Kehoe, A. Herz, M. Sakitt, B. Sechi-Zorn, N. Seeman and G. Snow, Phys. Rev. Letters 10, 409 (1963).
8. M. Bock, L. Lendinara, and L. Monari, Proc. Intern. Conf. High-Energy Phys., CERN, Geneva, 1962, 391.
9. M. Watson, M. Ferro-Luzzi and R. D. Tripp, Phys. Rev. 131, 2248 (1963).

FIGURE CAPTIONS

Fig. 1. Spark chamber arrangement for the detection of  $K^+$  produced from the polarized target.

Fig. 2. Beam optics. Not shown is a beam scraper at  $f_1$ .

Fig. 3.  $K^+$  range telescope. Objects labeled K and  $\mu$  are spark chambers, S and mu are scintillation counters, and C stands for Cerenkov water counter. A stopped  $K^+$  gives the signal

$$[S_1(SUM-S_2)S_3\bar{C}_1\bar{C}_2][C_T(SUM-MU)]_{\text{delayed}}$$

Fig. 4. Time spectrum of  $K^+$  decays.

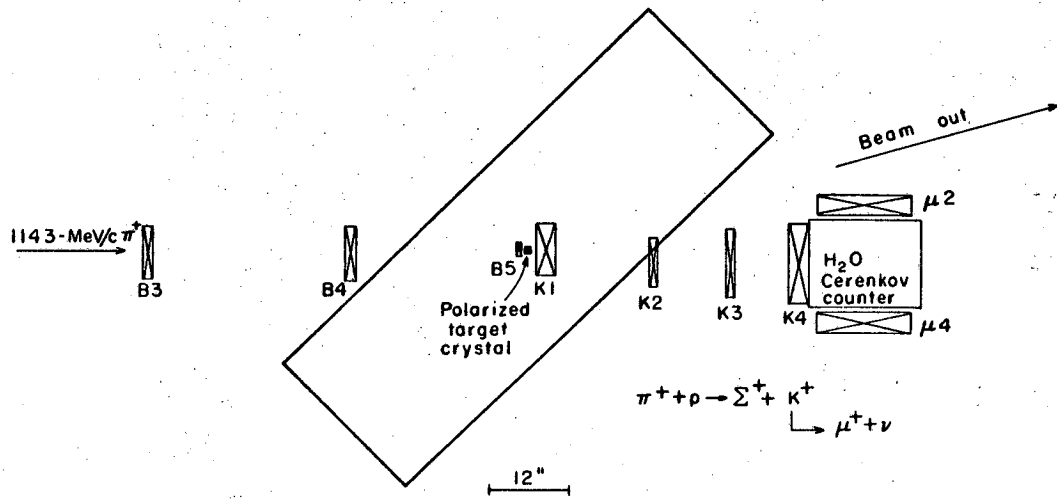
Fig. 5. Polarized target data. The dashed histogram is for negative target polarization (sigma and proton spins parallel) and the solid histogram is for positive target polarization.

Fig. 6.  $CH_2$  data. The dashed line is the result of a Monte Carlo calculation of  $K^+$  production from the carbon in the target.

Fig. 7. Asymmetry ( $\epsilon = \frac{N^+ - N^-}{N^+ + N^-}$ ) in data of Fig. 5 calculated for each 12 MeV bin in m.

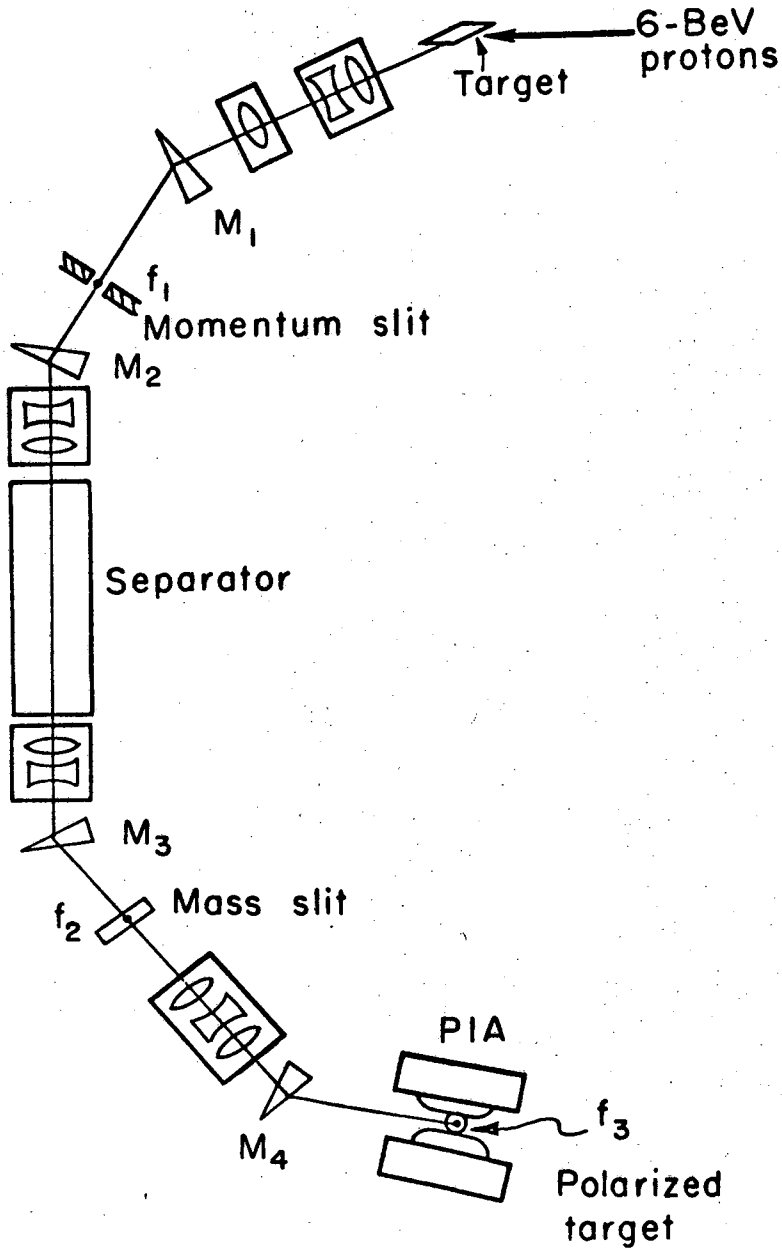
Fig. 8. Asymmetry ( $\epsilon = \frac{N^+ - N^-}{N^+ + N^-}$ ) in the polarized target data plotted in 4 MeV-wide bins.

Fig. 9. Comparison of the asymmetry observed in this experiment,  $\epsilon_{\text{exp}}$ , and the asymmetry predicted on the basis of polarization of sigmas produced in unpolarized hydrogen, with the requirements of odd or even  $K\Sigma N$  parity.



MUB14025

Fig. 1



MUB-13895

Fig. 2



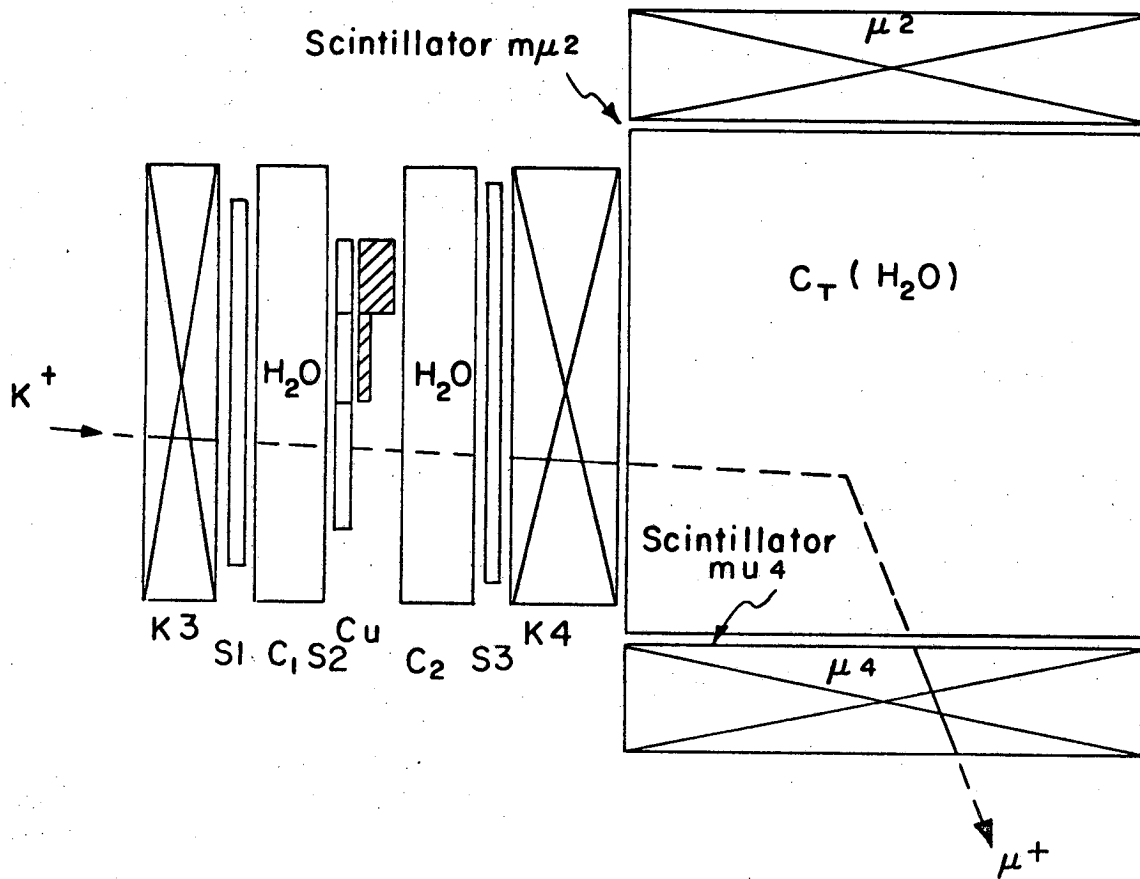
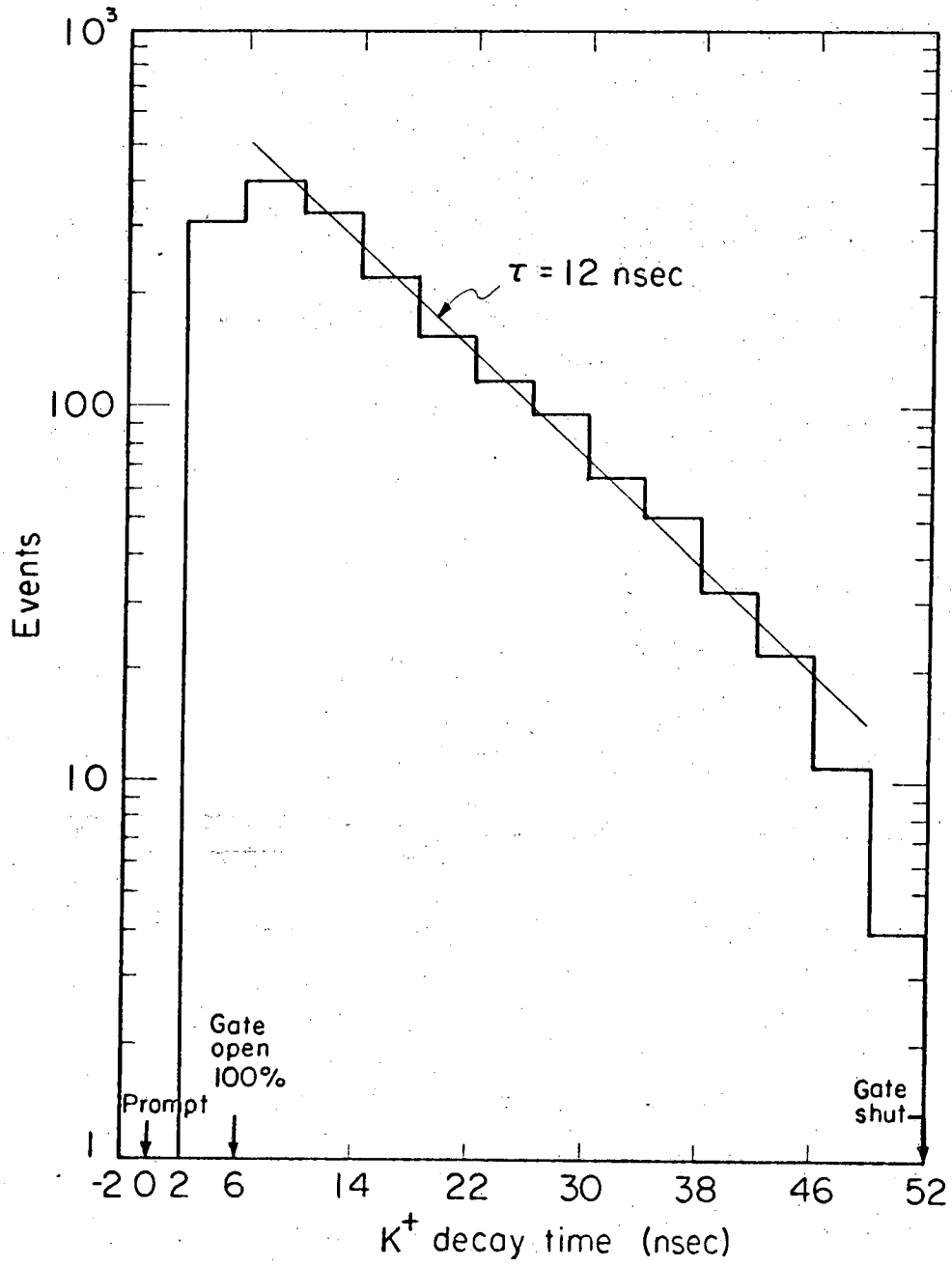


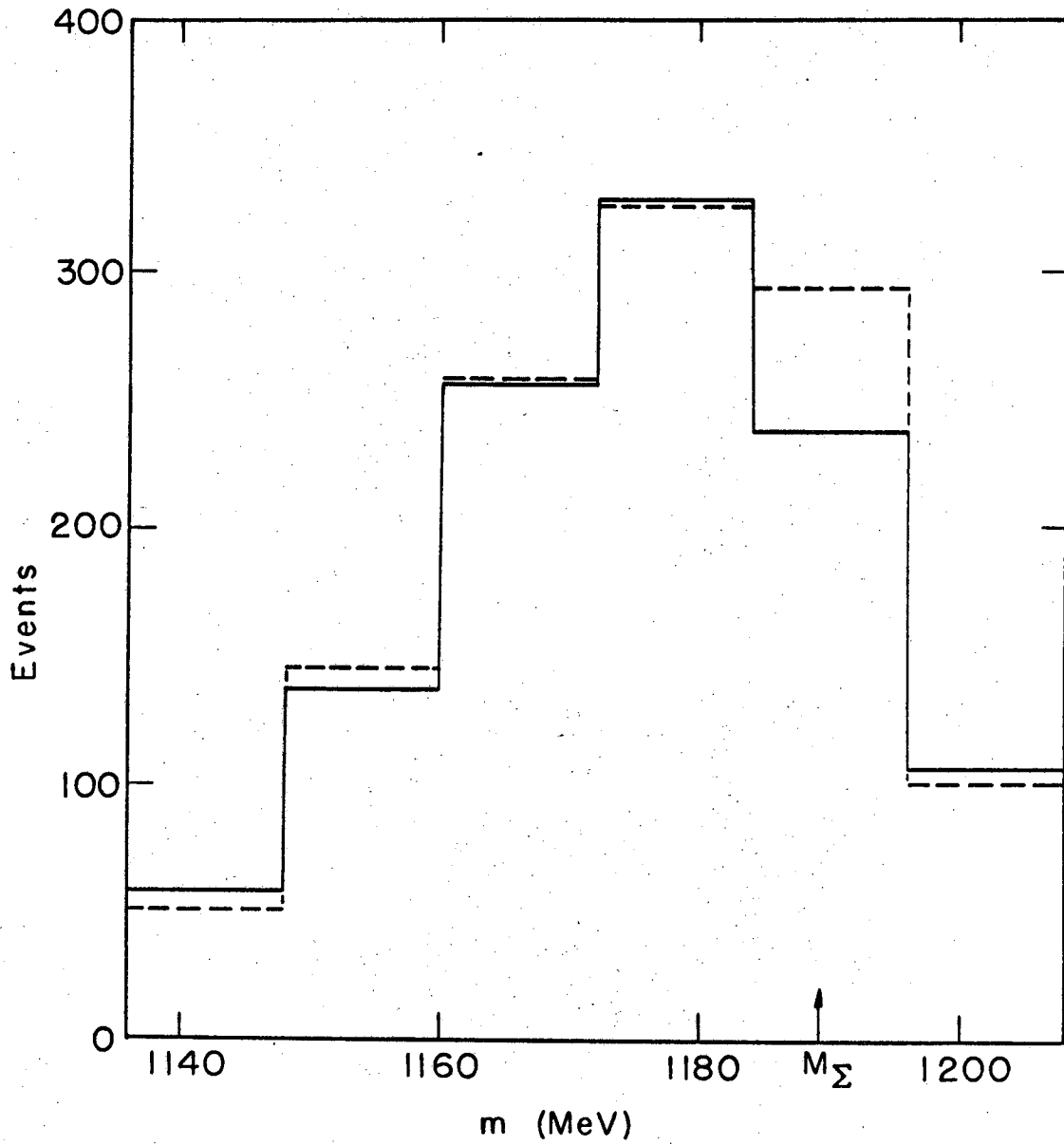
Fig. 3

MUB-13891



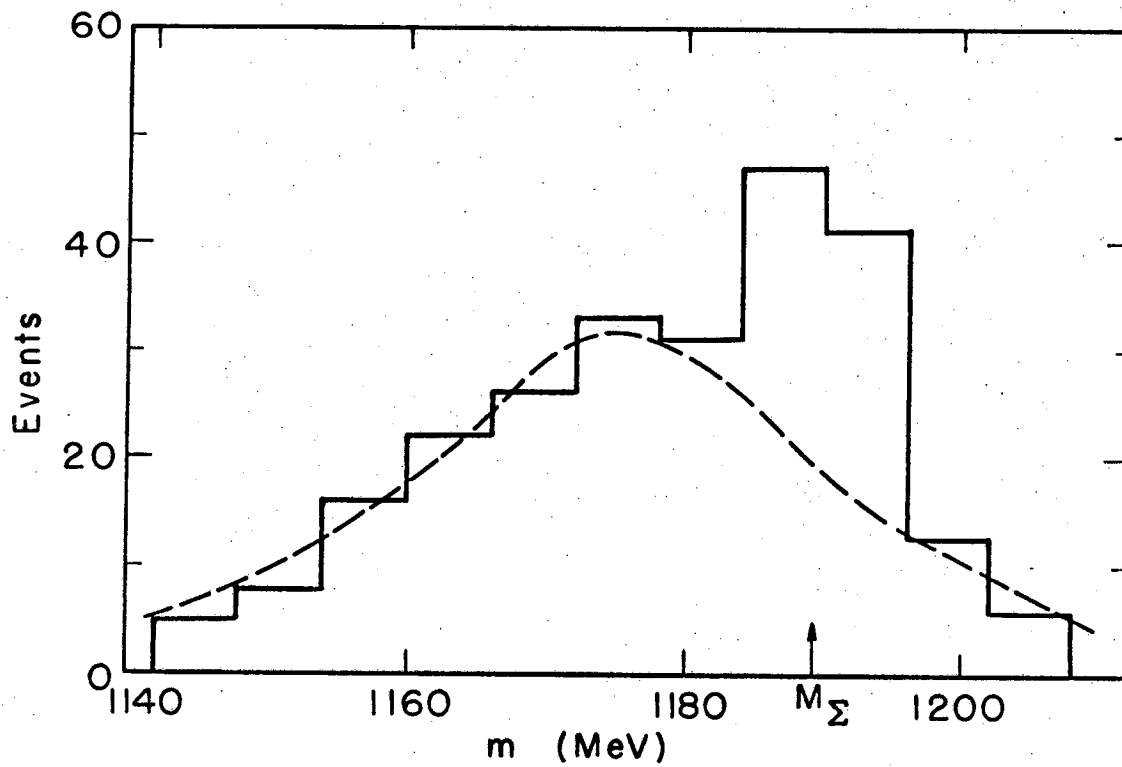
MUB-13894

Fig. 4



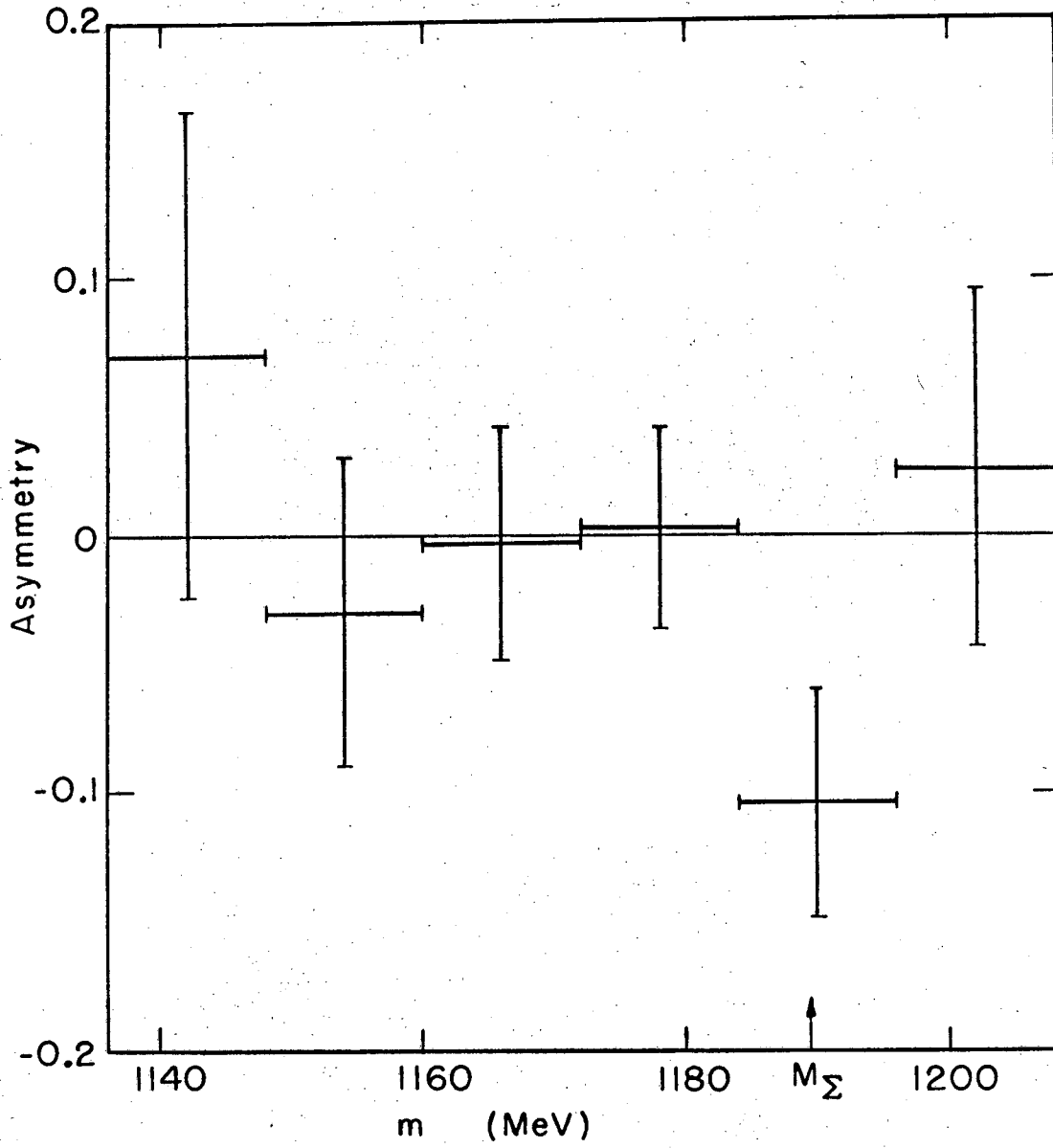
MUB-13765

Fig. 5



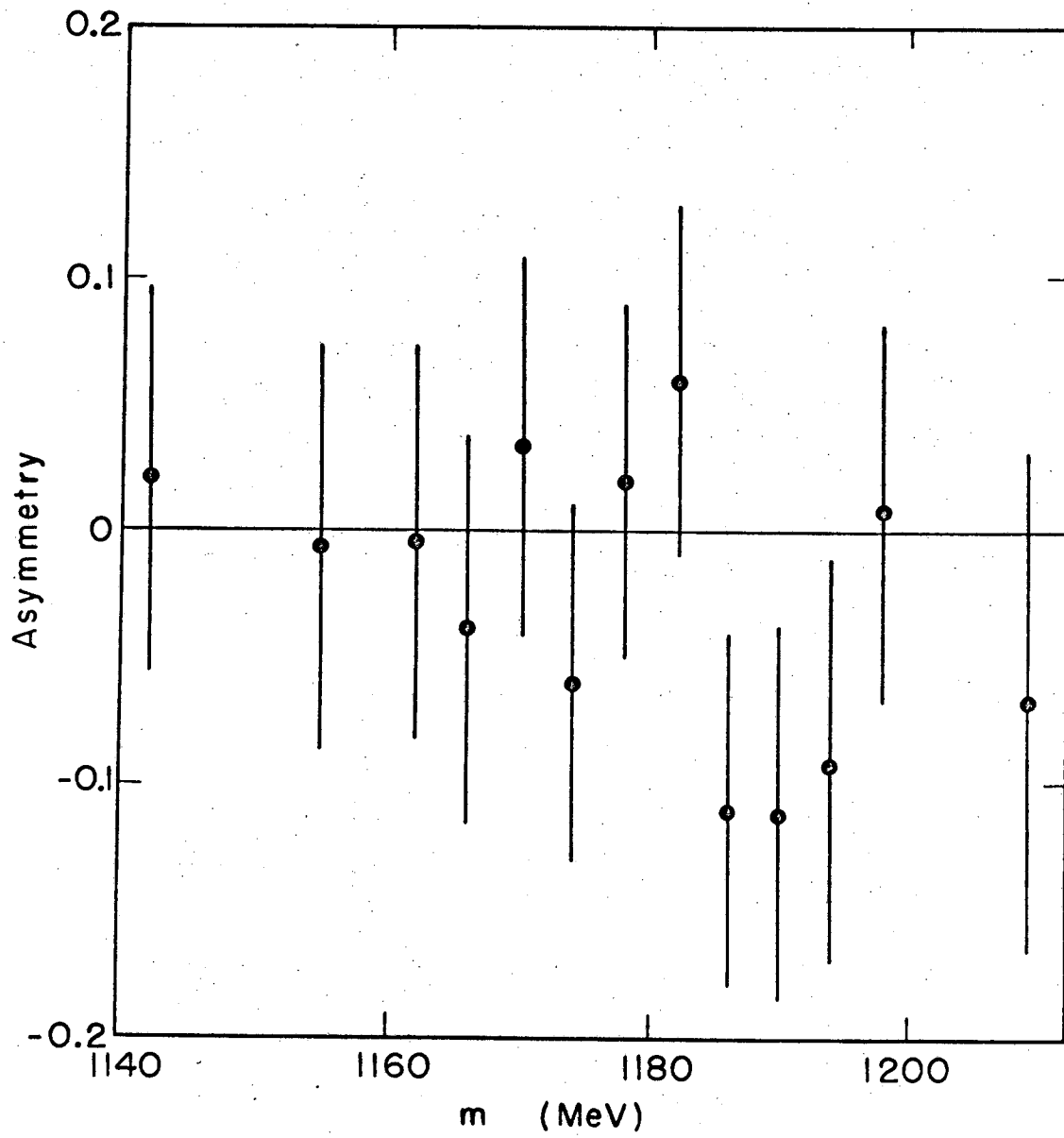
MUB13763

Fig. 6



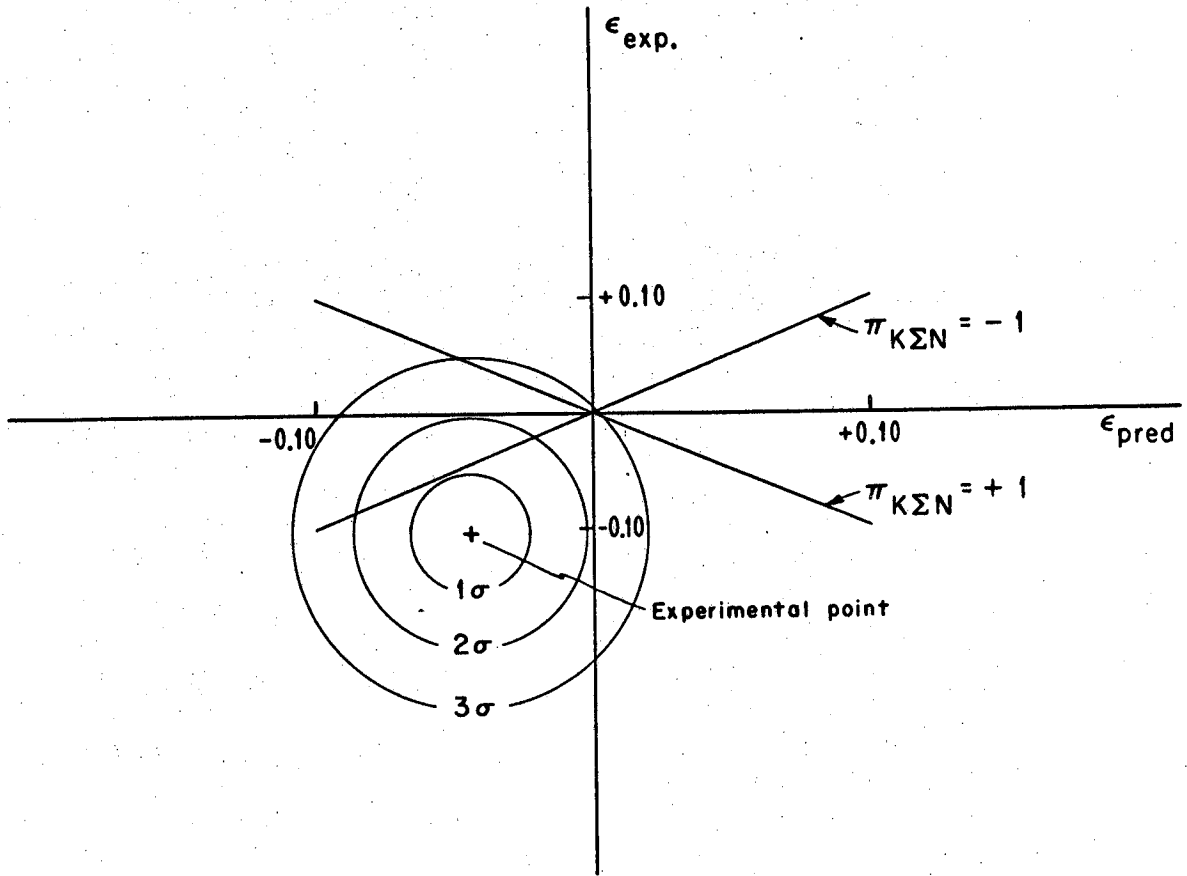
MUB-13762

Fig. 7



MUB-13764

Fig. 8



XBL670-5305

Fig. 9

This report was prepared as an account of Government-sponsored work. Neither the United States, nor the Commission, nor any person acting on behalf of the Commission:

- A. Makes any warranty or representation, expressed or implied, with respect to the accuracy, completeness, or usefulness of the information contained in this report, or that the use of any information, apparatus, method, or process disclosed in this report may not infringe privately owned rights; or
- B. Assumes any liabilities with respect to the use of, or for damages resulting from the use of any information, apparatus, method, or process disclosed in this report.

As used in the above, "person acting on behalf of the Commission" includes any employee or contractor of the Commission, or employee of such contractor, to the extent that such employee or contractor of the Commission, or employee of such contractor prepares, disseminates, or provides access to, any information pursuant to his employment or contract with the Commission, or his employment with such contractor.



